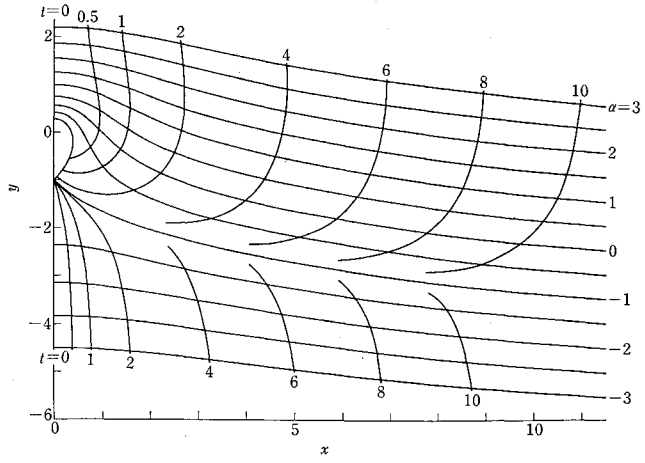


**Fig. 1 The irrotational flow past a vortex: streamlines and surfaces $t$ = constant. The latter are the shapes into which planes of fluid initially coincide with the plane $x = 0$ would be distorted as they passed over the vortex. Numerical results.**

the point on the $y$-axis at the time $t = 0$ and $r_1$ is the largest real root of the equations $r + \ln r = \alpha$ (for $\alpha > -1$) or $-r + \ln r = \alpha$ (for $\alpha < -1$). The integral in Eq. (13), however, cannot be carried out easily. We make, therefore, an approximation. The results of the numerical calculation for the positions of fluid particles on streamlines are shown in Fig. 1 as an illustration. These results are obtained by integrating Eqs. (6) and (7) numerically.

### Asymptotic Solution

The constant of motion $\alpha$, which has not been used in Corrsin's analysis, represents the remoteness of the path of the particle from the origin. Because we are considering the flow-field far from the origin, we can assume the values of $|\alpha|$ are very large.

For $|\alpha| \gg 1$, $r \geq r_1 = |\alpha| + O(\ln|\alpha|)$ and therefore $r \gg \ln r$ and we can neglect the terms of $\ln r$ comparing to $r$ in Eq. (13). Then, Eq. (13) can be approximated by

$$X = \int_{|\alpha|}^{r} \frac{(\alpha - \ln r)dr}{r(r^2 - \alpha^2)^{1/2}} \tag{14}$$

Integrating Eq. (14) by parts, we obtain

$$X = 1/|\alpha|\{(\pi/2)[\alpha - \ln(|\alpha|/2)] - (\alpha - \ln r)\,\text{arccosec}\,(r/|\alpha|) - I\} \tag{15}$$

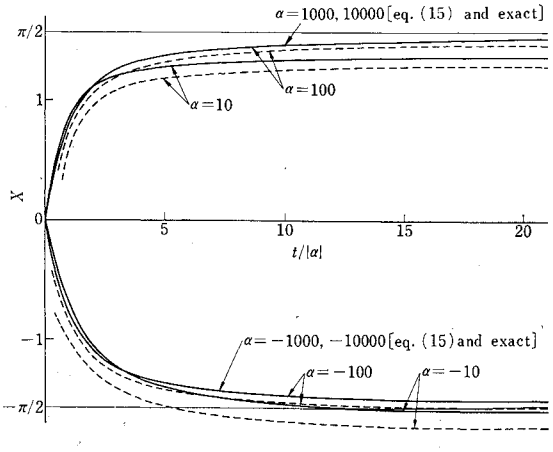


**Fig. 2 Variation of the drift $X$ for the flow past a vortex, along different streamlines, which are identified on the figure by the values of $\alpha$ noted on each curve. ——, exact numerical results; ------, approximate solution Eq. 15.**

where

$$I = \int_0^{|\alpha|/r} \frac{\arcsin\xi}{\xi}\,d\xi = (|\alpha|/r) + (1/2.3^2)(|\alpha|/r)^3 + (1.3/2.4.5^2)(|\alpha|/r)^5 + \ldots.$$

The total drift $X(\alpha)$ is obtained as

$$X(\alpha) = \lim_{r\to\infty} X = (\pi/2|\alpha|)[\alpha - \ln(|\alpha|/2)]$$

Taking into account the upstream-downstream symmetry, we get the distance for the $x$ separation of two fluid particles which start with zero $x$ separation far upstream, one passing far above the body, the other far below ($\alpha = \pm|\alpha|$, $|\alpha| \gg 1$)

$$x_U - x_L = 2(X_U - X_L) = 2\pi$$

This expression is independent of $\alpha$. Inverting this into the dimensional form by the definition (4), we have

$$x_U' - x_L' = \Gamma/U \tag{16}$$

This is just the conjecture given by Corrsin.[1] By the use of the Kutta-Joukowsky law, Eq. (16) relates particle displacement to lift $L$ per unit span by

$$x_U' - x_L' = L/\rho U^2$$

where $\rho$ is the density of the fluid. In Fig. 2, the approximate solution (15) is compared with the exact numerical solutions for several values of $\alpha$. The exact results are obtained by integrating Eqs. (6) and (7) numerically. The agreement is good for large values of $|\alpha|$.

### References

[1] Corrsin, S., "Conjecture on a Connection between Lift and Particle Displacement," *AIAA Journal*, Vol. 6, No. 9, Sept. 1968, pp. 1811–1812.

[2] Darwin, C. G., "Notes on Hydrodynamics," *Proceedings of the Cambridge Philosophical Society*, Vol. 49, Part 2, April 1953, pp. 342–354.

[3] Lighthill, M. J., "Drift," *Journal of Fluid Mechanics*, Vol. 1, Part 1, May 1956, pp. 31–53; also corrigenda, *Journal of Fluid Mechanics*, Vol. 2, Part 3, May 1957, pp. 311–312.

# Direct Measurement of the Thermal Conductivity of Shock Heated Argon

R. Ewald* and H. Grönig†
*Institut für Allgemeine Mechanik, Technische Hochschule, Aachen, Germany*

DESPITE a considerable amount of theoretical and experimental work on thermal conductivity of gases at elevated temperatures there is still a lack of its direct measurement. Almost all authors have assumed a thermal conductivity-temperature relationship according to $\lambda \sim T^\sigma$ (Refs. 1–5). This relationship then served to determine $\sigma$ experimentally. The general procedure applied by all these authors has been to calculate the thermal boundary-layer equations using

$$\lambda = \lambda_0(T/T_0)^\sigma$$

where $\lambda_0$ represents the known thermal conductivity at a reference temperature $T_0$. They then vary $\sigma$ until the mea-

Received October 3, 1970; revision received November 18, 1970.

* Research Scientist; now at Ernst-Mach-Institut für Stosswellenforschung, Freiburg, Germany.

† Professor of High-Temperature Gasdynamic. Member AIAA.

sured and calculated heat flux[1–4] or temperature profiles[5] coincide, provided that $\sigma$ is independent of the temperature. Another approach is followed by Smeets[6] who used a step-by-step procedure by determining the value of $\lambda$ at a certain temperature from its value at a lower temperature and the measured temperature profile of the boundary layer.

This paper deals with a direct method of obtaining $\lambda(T)$ from the experiment. Similar to all the other measurements the region behind the reflected shock at the end wall of a shock tube has been used as a test section. The basic idea of the method applied here is to follow the temperature boundary layer by a series of time-resolved interferograms obtained by a Mach-Zehnder interferometer with a high-frequency laser-stroboscope as a light source.

The basic relation follows from the conservation equations of mass and energy:

$$(\partial\rho/\partial t) + \partial(\rho u)/\partial x = 0 \tag{1}$$

$$\rho[(\partial h/\partial t) + u\,\partial h/\partial x] = \partial/\partial x(\lambda\,\partial T/\partial x) \tag{2}$$

where $x$ is the coordinate normal to the end wall, $u$ the flow velocity in this direction, $\lambda$ the heat conductivity, $h$, $T$, and $\rho$ the specific enthalpy, temperature, and density, respectively.

The following assumptions lead to Eqs. (1) and (2): the problem is regarded one-dimensional since the width of the shock tube (56.4 mm) is large compared to the boundary layers at the side walls; the pressure is assumed constant and the flow velocity small, thus, the momentum equation includes quantities of higher order.

The specific heat of argon $c_p$ below 5000°K at a pressure higher than 20 torr is constant within less than 0.01%[7] with a degree of ionization a below $10^{-4}$%. Therefore, with

$$dh = c_p dt \tag{3}$$

and

$$\rho T = \text{const} \tag{4}$$

inserted into Eqs. (1) and (2) yields the following relation for $\lambda$:

$$\lambda = \lambda^{(1)} + \Delta\lambda^{(2)} + \Delta\lambda^{(3)} \tag{5}$$

with

$$\lambda^{(1)} = \rho c_p(\partial T/\partial t)/(\partial^2 T/\partial x^2) \tag{6}$$

$$\Delta\lambda^{(2)} = \rho c_p u(\partial T/\partial x)/(\partial^2 T/\partial x^2) \tag{7}$$

or by making use of Eq. (1)

$$\Delta\lambda^{(2)} = c_p \frac{\partial T}{\partial x}\int_0^x \frac{\rho}{T}\frac{\partial T}{\partial t}\,dx \Big/ \frac{\partial^2 T}{\partial x^2} \tag{8}$$

$$\Delta\lambda^{(3)} = -\,d\lambda/dT(\partial T/\partial x)^2/\partial^2 T/\partial x^2 \tag{9}$$

$\lambda^{(1)}$ represents the first order expression for the thermal conductivity. Since the flow velocity $u$ is small, $\Delta\lambda^{(2)}$ turns out as a positive additional term of approximately 20%. $\Delta\lambda^{(3)}$ is a small correction of about 2% resulting from the temperature dependence of the heat conductivity. For the evaluation of the numerical value of this last term, $\Delta\lambda^{(3)}$, only, the temperature dependence has been assumed to $\lambda \sim T^{\sigma}$ ($\sigma = \frac{2}{3}$).

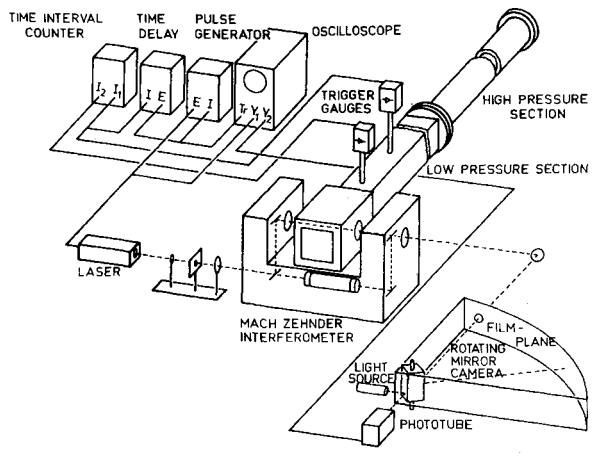


**Fig. 1 The experimental apparatus.**

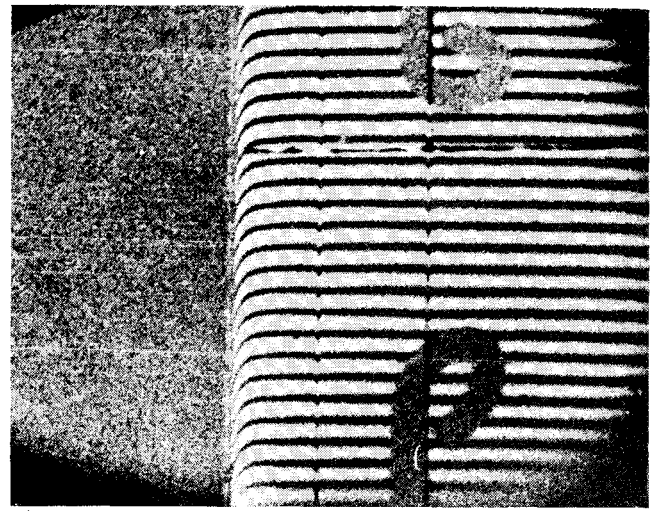

**Fig. 2 Interferogram with a dark zone due to the density gradient. The thin parallel lines and hooks are for aligning purposes.**

All quantities in Eqs. (5–9) can now be determined from the interferometric records provided that time and space resolved measurements are available. This has been achieved by the experimental set-up shown schematically in Fig. 1. The density variations near the end wall of the shock tube are measured by a Mach-Zehnder interferometer together with a ruby-laser stroboscope[8] and a free-running rotating mirror camera. The laser stroboscope could be programed to emit a series of light pulses during a present time with frequencies from 10 kc up to more than 1 mc. The noncontinuously writing camera had an exposure probability of nearly 50%; an excessive film waste could be avoided by monitoring the position of the rotating mirror by a pilot lamp and a phototube on a scope to show whether the film had been exposed.

Figure 2 shows a single photograph from a series taken at a laser pulse frequency of 45 kc with an exposure time of 50 ns. (The film material was Kodak High Speed Infrared film HIR 121-1.) The dark zone immediately ahead of the wall is due to the density gradient refracting the originally parallel light beam towards the wall.

From a series of interferograms similar to that of Fig. 2 the density distribution as a function of the distance from the end

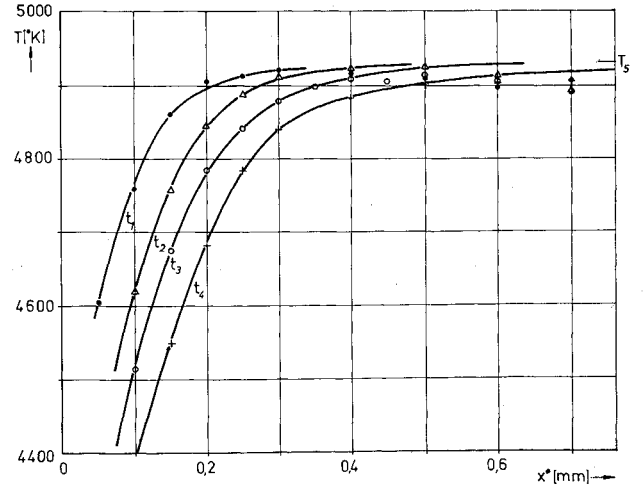


**Fig. 3 Distribution of temperature at different times.**

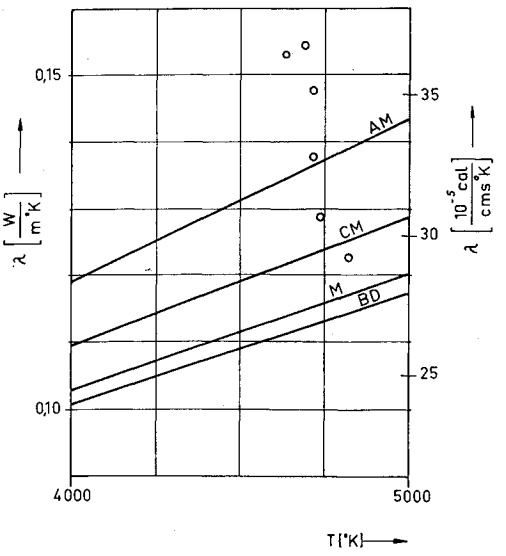


**Fig. 4 Heat conductivity, directly measured and theoretical values; AM: Amdur, Mason,[9] CM: Collings, Menard,[2] M: Matula,[4] BD: Bunting, Devoto.[5]**

wall had been obtained for several times after the reflection of the shock. The results of this evaluation are given in Fig. 3 which shows the temperature boundary layer at the end wall for four different times, i.e., $t_1 = 60$ $\mu$s, $t_2 = 120$ $\mu$s, $t_3 = 180$ $\mu$s, and $t_4 = 300$ $\mu$s after the reflection of the shock; $x$ represents the distance from the wall measured on the film.

From these temperature profiles the derivatives with respect to space and time are calculated. For this purpose the curves in Fig. 3 are approximated by polynomials which are adapted to the curves by a procedure involving an integration step in order to get smooth functions for differentiation. Using these functions the thermal conductivity $\lambda$ is calculated from Eqs. (5–9) for several distances $x$ from the end wall, representing simultaneously several slightly different temperatures. Results of this procedure for a series of experiments are given in Fig. 4 together with results obtained by former authors using the potential law $\lambda \sim T^{\sigma}$ with different values of $\sigma$.

An estimate shows that the maximum error is of the order of $\pm 20\%$. The main part of this error is due to the differentiation procedure involved in the numerical evaluation. The scattering of the experimental results has the same range as found with the potential law results mentioned. Therefore, in this way no decision can be made to support one of the cited measurements. The main aim of this Note is to present a new method to measure directly the thermal conductivity of gases. The first preliminary experimental results show that this method provides an accuracy at least comparable with the indirect measurements.

### References

[1] Smiley, E. F., "The Measurement of the Thermal Conductivity of Gases at High Temperatures with a Shock Tube: Experimental Results in Argon at Temperatures between 1000°K and 3000°K," Ph.D. thesis, 1957, Catholic University of America, Washington, D. C.

[2] Collins, D. J. and Menard, W. A., "Measurements of Thermal Conductivity of Noble Gases in the Temperature Range 1500 to 5000°K," *Journal of Heat Transfer*, Vol. C 88, No. 1, Feb. 1966, pp. 52–56.

[3] Camac, M. and Feinberg, R. M., "Thermal Conductivity of Argon at High Temperatures," *Journal of Fluid Mechanics*, Vol. 21, Pt. 4, April 1965, pp. 673–688.

[4] Matula, R. A., "High Temperature Thermal Conductivity of Rare Gases and Gas Mixtures," *Journal of Heat Transfer*, Vol. C 90, No. 3, Aug. 1968, pp. 319–327.

[5] Bunting, J. O. and Devoto, R. S., "Shock Tube Study of the Thermal Conductivity of Argon," SUDAAR 313, July 1967, Dept. of Aeronautics and Astronautics, Stanford University, Palo Alto, Calif.

[6] Smeets, G., "Bestimmung der Wärmeleitfähigkeit heisser Gase aus der Temperaturgrenzschicht im Stossrohr," *Zeitschrift fuer Naturforschung*, Vol. 20a, No. 5, May 1965, pp. 683–689.

[7] Hilsenrath, J., Messina, C. G., and Klein, M., "Table of Thermodynamic Properties and Chemical Composition of Argon in Chemical Equilibrium, Including Second Virial Corrections, from 2400°K to 35000°K," AEDC-TR-66-248, Dec. 1966, Arnold Engineering Development Center, Arnold Air Force Base, Tenn.

[8] Alfs, A., "Erzeugung einer kleinen Serie von partiellen Rubinlaser-Riesenpulsen," *Proceedings of the 8th International Congress on High-Speed Photography*, Wiley, New York, 1968, pp. 281–283.

[9] Amdur, I. and Mason, E. A., "Properties of Gases at Very High Temperatures," *The Physics of Fluids*, Vol. 1, No. 5, Sept.–Oct. 1958, pp. 370–383.

# Earth Escape Regions near the Moon

J. PIKE*
*Royal Aircraft Establishment, Bedford, England*

SPACECRAFT powered by microthrust may find it convenient to escape Earth by use of the moon's attraction. A method of achieving this which has previously been considered[1] is to orbit the spacecraft round the Earth in a direction contrary to that of the moon. A near miss of the moon is then just sufficient to attain escape velocity. A disadvantage of the contra-rotating orbit is that the Earth's axial spin makes it more difficult to place a spacecraft in its initial "near Earth" orbit.

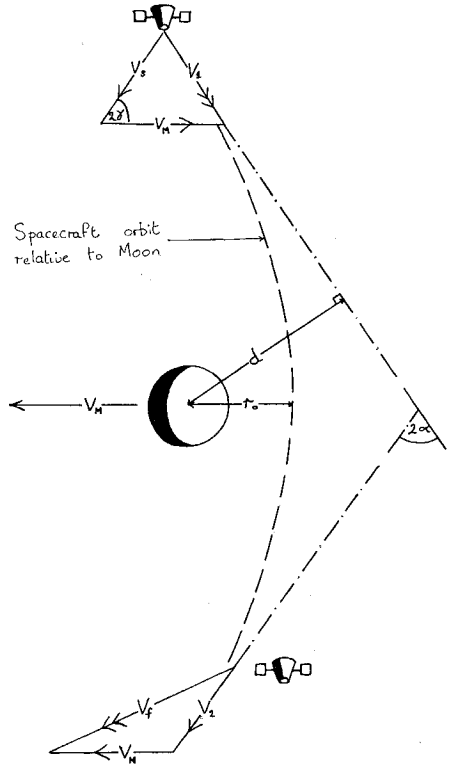


**Fig. 1 Spacecraft orbit about moon.**

Received May 26, 1970. The basis of this work was done while the author was at the College of Aeronautics, Cranfield, England.

* Senior Scientific Officer.